To appear in Artificial Intelligence in Medicine (1998)
Special Issue on Modeling Brain Disorders

Neuromodulatory control of hippocampal function: Towards a model of Alzheimer's disease

Elliot D. Menschik [a] and Leif H. Finkel [a,b]

[a]*Institute of Neurological Sciences* and [b]*Department of Bioengineering*
301 Hayden Hall, 3320 Smith Walk, University of Pennsylvania
Philadelphia, Pennsylvania 19104, USA
menschik@jupiter.seas.upenn.edu
leif@jupiter.seas.upenn.edu

Submitted April 1997; revised October 1997

Abstract

Alzheimer's disease (AD) is a progressive neurodegenerative disorder of cognitive function whose cellular pathology and molecular etiology have been increasingly and dramatically unraveled over the last several years. Despite this substantial knowledge base, the disease remains poorly understood due to a basic lack of understanding of how memories are stored and recalled in the brain. We describe a preliminary attempt at constructing a detailed model of these basic neural mechanisms; in particular, the natural dynamics of neuronal activity in hippocampal region CA3 and the modulation and control of these dynamics by subcortical cholinergic and GABAergic input to the hippocampus. We view the construction of such a model, with sufficient detail at the cellular and subcellular level, to be a necessary first step in understanding the effect of AD pathology on the functional behavior of the underlying neural circuitry.

The network is based on the 66-compartment hippocampal pyramidal cell model of Traub and colleagues [70] and their 51-compartment interneuron [72] interconnected with realistic AMPA-, NMDA-, and $GABA_A$-mediated synapses. Traub and others [14, 74, 79] have shown that a network composed of these modeled cells is capable of synchronization in the gamma frequency range. We demonstrate here that this synchronization mechanism can implement an attractor-based autoassociative memory. A new input pattern arrives at the beginning of each theta cycle (comprised of 5-10 gamma cycles), and the pattern of activity across the network converges, over several gamma cycles, to a stable attractor that represents the stored memory.

In this model, cholinergic deprivation, one of the hallmarks of AD, leads to a slowing of the gamma frequency which reduces the number of "cycles" available to reach an attractor state. We suggest that this may be one mechanism underlying the memory loss and cognitive slowing seen in AD. Our results also support the idea that acetylcholine acts on individual neurons to induce and maintain a transition from intrinsic bursting to spiking in pyramidal cells [54]. These results are consistent with the hypothesis that spiking and bursting in CA3 pyramidal cells mediate separate behavioral functions [15], and that cholinergic input is required for the transition to and support of behavioral states associated with the online processing and recall of information.

Keywords: hippocampus; CA3; acetylcholine; interneurons; oscillations; Alzheimer's disease

1. Introduction

1.1 Hippocampal disease and neuromodulation

The hippocampus has been a major focus of both basic and clinical neuroscience research, the latter stemming from its central role in Alzheimer's disease (AD), temporal lobe epilepsy, and traumatic brain injury. The hippocampal formation is the region first and most severely damaged in Alzheimer's disease as revealed by the onset of neuritic plaques and neurofibrillary tangles [44, 46, 59, 63]. Recent work in AD has focused on linking the pathology to neurotoxicity and trauma and investigating the underlying molecular genetics of the disease. A second major area of AD research has been the investigation of the subcortical pathology that strips archicortical and neocortical structures of their regulatory neuromodulators. It has been suggested that specific perturbations of neuromodulatory agents, particularly acetylcholine (ACh), may play a role in the behavioral dysfunction of Alzheimer's disease [80, 81].

The early impairment of memory in AD is usually attributed to pathologic changes occurring in hippocampal region CA1, the adjacent subiculum, and entorhinal cortex [3, 10, 44]. Hippocampal region CA3 appears to be spared initially, however damage to subcortical neuromodulatory sources may have important consequences for the function of CA3 that are not apparent from the histopathological studies. We propose that subcortical neuromodulation, together with certain classes of hippocampal interneurons, serve as a control structure that regulates the function of the hippocampus [25], and we develop a model of the role of this control structure in AD. We suggest that understanding the properties of such neuronal regulation and control is critical for understanding the cellular underpinnings of AD.

For over twenty years, it has been known that the AD-afflicted brain is associated with a significant decline in levels of choline acetyltransferase (ChAT), the enzyme that synthesizes ACh [8, 22]. The deficit in ChAT attracted much attention since it had long been known that centrally acting anti-cholinergic drugs such as scopolamine impaired recent memory (see [23]). It made sense that a deficiency of ACh might be associated with memory impairment, and it was hoped that pharmacological therapies might increase ACh levels in the brain thereby improving cognitive function in AD. The limited efficacy of acetylcholinesterase inhibitors underscores the necessity of understanding the role of the cholinergic deficit in AD as well as a knowledge of the normal role of ACh in information processing and memory storage.

1.2 Cholinergic neuromodulation of single cells

Cholinergic inputs to hippocampus originate from the medial septal nuclei and the vertical limb of the diagonal band of Broca. Acting through muscarinic receptors, ACh is known to affect the ionic currents, membrane potential, spike frequency adaptation, and synaptic efficacy of pyramidal cells and inhibitory interneurons.

At the cellular level, ACh exerts effects on both potassium and calcium channels via muscarinic receptors. In hippocampal pyramidal cells, muscarinic agonists have been reported to decrease I_{AHP} [17-19, 51], decrease I_A [58], decrease I_M [11], and decrease a resting K^+ current [7, 12, 51]. Several studies have described muscarinic inhibition of calcium currents [26] where ACh appears to inhibit high-threshold channels and excite low-threshold channels [24, 67]. In the case of high-threshold channels, several different channel types demonstrate muscarinic inhibition [24, 68], and both voltage-dependent and voltage-independent components appear to exist [69]. It has been reported that ACh has similar effects on the array of ionic conductances in interneurons [25].

The muscarinic actions on individual ionic currents form the foundation for the generally "excitatory" physiological effects of ACh. In pyramidal cells, ACh causes a slow depolarization due to the suppression of a tonically active K^+ current [51]. ACh also suppresses spike frequency adaptation in pyramidal cells due to decreases in calcium-dependent K^+ currents and the M current [51]. In hippocampal interneurons, ACh causes a rapid excitation of the cell via modulation of a K^+ conductance [60].

Several studies have examined the synaptic effects of cholinergic neuromodulation as well (see [29] for review). ACh causes presynaptic suppression of excitatory synaptic transmission [43, 77] with a stronger effect in the stratum radiatum than in the stratum lacunosum-moleculare [33]. It also yields decreased mIPSCs most likely due to the high density of m2 receptors on terminals of those interneurons innervating the somata of pyramidal cells [25].

Taken together, these findings indicate that acetylcholine is known to alter a wide array of cellular properties, but the question remains as to the resulting effect on network *function*. The major effort in this direction has been made by Hasselmo and colleagues [4, 5, 30-34]. In their model, acetylcholine acts to switch between learning and recall of spike frequency patterns by suppressing synaptic transmission at the Schaffer collaterals or the recurrent collaterals of the stratum radiatum in favor of input from entorhinal cortex in the stratum lacunosum-moleculare. They propose that AD-related reductions in acetylcholine result in "synaptic runaway" where previously stored memories interfere with the formation of novel memories.

We propose here a complementary hypothesis based on the effects of acetylcholine on several important ionic conductances of pyramidal cells and upon the role of interneurons. In particular, we suggest that acetylcholine regulates the transition between bursting and spiking behavior in hippocampal, intrinsically bursting pyramidal cells. Physiological studies of neuromodulation in hippocampus, neocortex, and thalamus have led McCormick to argue that acetylcholine contributes to the control of neuronal activity and the sleep-wake cycle [53, 54]. We extend this assertion by proposing that memory coding, storage and recall make use of different spiking regimes in the hippocampus. This hypothesis is compatible with the "two-stage" model of memory advocated by Buzsáki [15]. In particular, we propose that mnemonic recall involves the convergence of cellular activity to a stored attractor state under the control structure imposed by gamma and theta-band oscillatory activity.

1.3 A biological autoassociative attractor network

The network we have chosen to construct and investigate is a biological implementation of the Hopfield formalism for attractor neural networks [1, 38]. Attractor models have provided the basis for several previous hippocampal-based models of memory and spatial navigation. Similarly, it has been the foundation for a number of studies of AD [40, 41, 61, 62] and has been a useful tool for exploring the consequences of neuronal death and synaptic perturbation.

While the simplicity of such models allows for analytical tractability and a certain elegance, for several reasons we feel that it is critical that computational studies of AD utilize realistic cellular-level models along with the appropriate anatomy. First, in order to understand or predict the functional consequences of pathology occurring at the cellular or subcellular level, detailed models are required. Not all pathology leads to cell death nor to synaptic perturbations. There are undoubtedly more subtle, yet highly significant influences on network function that are not apparent in histopathological studies. Second, it is most likely that therapeutic innovations will have to target the cellular and subcellular foundations of the disease; an understanding of these processes and how they can be manipulated is critical. Third, the applicability of the attractor neural network to biological neurons has not been convincingly demonstrated.

If attractor networks do have a biological analog, the CA3 region of the hippocampus appears to be a natural neuronal substrate [76] due to its unique recurrent connectivity and dual-perforant path/mossy fiber inputs. The functional architecture of our network is schematized in Fig. 1. Mnemonic information is assumed to be encoded as the spatially-distributed pattern of temporally-precise single pyramidal cell spikes across the CA3 region. The network state is defined as the spatial pattern of spikes during a time window consisting of single gamma-cycle. In addition, the theta rhythm provides a clocking mechanism for entorhinal-based input of new patterns to the network for recall of stored memories. After the transient inputs are received at the beginning of a theta cycle, the dynamics of pyramidal cell spiking are directed by the recurrent synaptic matrix until either a fixed-point attractor state or the end of half the theta cycle is reached.

2. Methods

2.1 Software and Hardware

Compartmental simulations were constructed using the GENESIS development package [9] and PGENESIS, its recent implementation for parallel platforms [27]. Simulations were performed on a four-processor Silicon Graphics Origin2000. Differential equations were solved using Crank-Nicholson implicit integration with a step size of 25μs. This value was determined to be the largest step size that still allowed

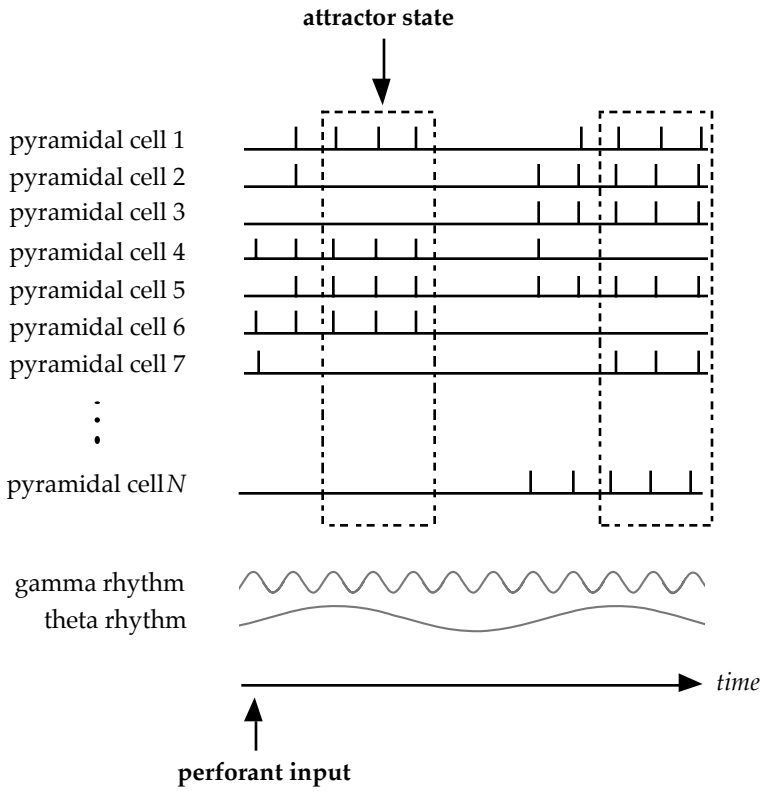

Fig. 1. Schematic of the biological analog of an autoassociative attractor neural network. Shown are hypothetical spike traces of CA3 pyramidal cells with idealized gamma (42 Hz) and theta (6 Hz) population rhythms shown for reference. The state of the network is defined by the spatial pattern of spikes during each gamma cycle. This gamma-band synchronization is induced by a network of mutually inhibitory interneurons which constrain spikes to windows of 25 ms or so. In contrast, slower theta-band oscillations, induced by septal interneurons, are responsible for clocking new perforant input to the network from entorhinal cortex. The recurrent synapses direct the activity of the pyramidal cells to the stable network state that corresponds to a stored pattern (a fixed-point attractor). The network is reset during the second half of the theta rhythm by high-frequency inhibition.

for accurate convergence. Simulations of artificial neural networks were performed using Mathsoft's MATLAB while nonlinear curve fitting was performed using Wolfram Research's *Mathematica*.

2.2 Cellular models and synapses

The individual cells used in the network simulations are the 66-compartment hippocampal CA3 pyramidal cell [70] and the 51-compartment hippocampal interneuron [72] developed by Traub and colleagues. Although they are far from a complete description of the cellular and subcellular biophysics of actual cells, these two models remain the most biologically realistic hippocampal models published to date in terms of their array of cellular components, morphological structure (e.g. branching dendrites, axon initial segments, axons), and fidelity to cellular physiology as recorded*in vitro* and *in vivo*. The model cells contain a wide array of voltage-, time- and/or concentration-dependention channels to endow the cell with the fast sodium current (I_{Na}), delayed-rectifierpotassium current (I_K), transient potassium current (I_A), calcium-dependentpotassium current (I_C), afterhyperpolarizing calcium-dependentpotassium current (I_{AHP}), and high-threshold calcium current (I_{Ca}). The pyramidal cell is the same as the one previously ported to GENESIS by Sampat and Huerta (available to members of the BABEL user group at ftp://babel.bbb.caltech.edu) with the exception that the afterhyperpolarization conductance density was

decreasedby 25% (as describedby Traub et al. [73]). Porting the interneuron model to GENESIS was a straightforward task and we then used the model as both a basket cell and a chandelier cell (again as in [73]).

The synaptic receptors' kinetics and somatodendritic locations are implemented as described by Traub and colleagues for α-amino-3-hydroxy-5-methyl-4-isoxazole proprionic acid (AMPA), *N*-methyl-*D*-aspartate (NMDA), and γ-amino-butyric acid type A ($GABA_A$) receptors [73]. AMPA and NMDA receptors always colocalize to the same synapse. The only notable modification is the use of a dual exponential function for NMDA and $GABA_A$ conductances

$$g_{syn}(t) = \bar{g}_{syn} \cdot A \cdot \left(e^{-\frac{t}{\tau_{syn1}}} - e^{-\frac{t}{\tau_{syn2}}} \right) \quad (1)$$

where $\bar{g}_{syn}$ is the maximal synaptic conductance and A is the normalization constant. The time constants were fitted to match the time-courses of the original functions proposed by Traub et al. [73]. Specifically, pyramidal cell NMDA conductances had a 5 ms time-to-peak and a decay time constant of 150 ms (τ_{syn1} = 144 ms; τ_{syn2} = 1 ms) while interneurons had a 60 ms decay time constant (τ_{syn1} = 54 ms; τ_{syn2} = 1.3 ms). $GABA_A$ conductances on both pyramidal cells and interneurons had nearly-instantaneous time-to-peak and a decay time constant of 10 ms (τ_{syn1} = 9.4 ms; τ_{syn2} = 0.1 ms).

2.3 Network Connectivity

In constructing the model network we attempted to be as faithful as possible to known hippocampal anatomy; the result is sketched in Fig. 2. CA3 pyramidal cells and interneurons are modeled explicitly while inputs from the entorhinal cortex and the medial septal nuclei are modeled as spike trains and graded neuromodulation respectively. The network is comprised of 136 cells: 64 pyramidal cells, 8 basket cells, and 64 chandelier cells [25].

The network of model basket cells is responsible for the generation of gamma-band (40-100 Hz) synchronized oscillations by mutual inhibition, as has been previously described [14, 74, 79]. The basket cells project to each other in an all-to-all fashion with each synapse making a single perisomatic contact with a maximal $GABA_A$ conductance of 4.875 nS. The basket cells also project to the pyramidal cells in an all-to-all fashion with each presynaptic fiber making contact on each of the postsynaptic perisomatic compartments containing $GABA_A$ receptors for a total 4 nS conductance over this region. These interneurons received input from 1) all pyramidal cells which make synaptic contacts on a compartment containing AMPA and NMDA receptors with maximal conductances of 0.5 nS and 0.125 nS respectively 2) septal GABAergic "theta-bursting" neurons providing theta-band (6-10 Hz) rhythmic inhibition [78] and 3) diffuse septal cholinergic input. The theta-band inhibition was represented in the model by a 6 Hz square wave of somatic current injection with 1.125 nA amplitude. The cholinergic input is described below.

Perforant path input was via AMPA- and NMDA- mediated synapses in the most distal dendrites of the pyramidal cell model (stratum lacunosum-moleculare) with maximal conductances of 4.4 nS and 11.776 nS respectively. Perforant input was generated as a spatial pattern of spikes at the presynaptic terminals.

Since this is a preliminary investigation, we have chosen to begin with a pre-wired network storing arbitrarily chosen memories. This is intended to be an approximation of a more biologically-relevant network that would have already undergone Hebbian associative learning, presumably via LTP and LTD. The exploration of a network with the capacity to both learn and recall has been deferred for later study. We chose five random 64-bit binary strings ξ to store as memories, shown below:

$$\begin{aligned}
&1100010111011101101001001001001110010010001110100100101000010111\\
&1101100101010001010110001010100101110111101100001100010111001101\\
&1010111010110110110001100000011110110000100100001011100011101100\\
&1110000111010011000010011100000100111110100011011011110100101111\\
&1010011001101101001001110110001101000111101111011001000000011010
\end{aligned}$$

The fixed connectivity of the recurrent synapses was determined using Hopfield's algorithm for storing binary patterns in an attractor neural network [38] of N neurons where the NxN elements of the synaptic matrix T are a function of the p different patterns ξ.

$$T_{ij} = \begin{cases} \sum_p \xi_i^p \xi_j^p, & i \neq j \\ 0, & i = j \end{cases} \tag{2}$$

This connectivity was tested in a 64-cell *artificial* Hopfield network to verify the rapid and robust autoassociative recall abilities of the network for these patterns. The artificial neural network was found to converge rapidly (within 5 synchronous updating cycles) to each of the stored patterns. The network was also able to tolerate a high degree of input pattern corruption and still converge to the proper uncorrupted pattern (data not shown).

The synaptic matrix is implemented in the biological model using AMPA- and NMDA-mediated synapses of the recurrent collaterals in the stratum radiatum for positive T_{ij} values and $GABA_A$-mediated synapses on the axonal initial segment (via chandelier cells) for negative ones. The actual T_{ij} value is used to scale the maximal conductances of the receptors (0.55 nS for pyramidal cell AMPA, 0.736 nS for pyramidal cell NMDA, and 3 nS for pyramidal cell axonal $GABA_A$) while chandelier cell AMPA and

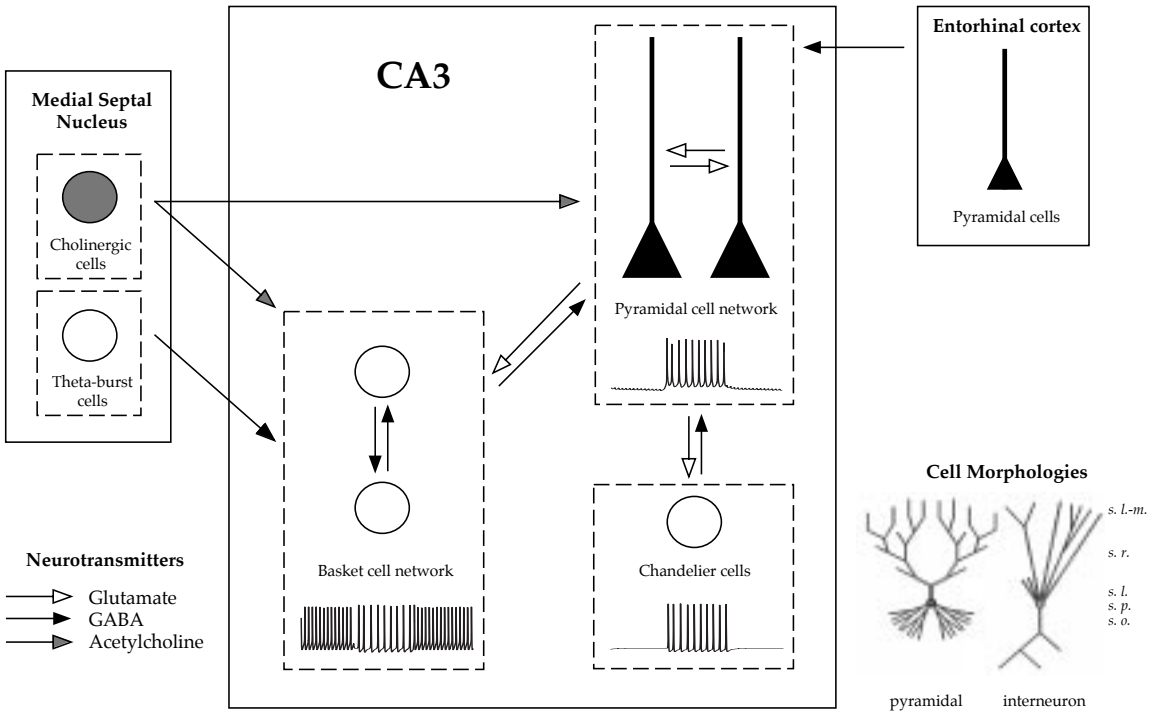

Fig. 2. The architecture and behavior of the model is consistent with known hippocampal anatomy and physiology. Shown is a network schematic and sample somatic voltage traces from the three CA3 cell populations. Mutually inhibitory basket cells are depolarized by septal cholinergic and local pyramidal cell glutamatergic input while being simultaneously inhibited by septal perisomatic GABAergic input oscillating at theta frequencies. The inhibition between basket cells creates synchronous gamma oscillations which are themselves modulated at theta frequencies by the septal inhibition. CA3 pyramidal cells are depolarized in the *s. p.* by septal cholinergic input, in the *s. r.* by recurrent glutamatergic input, and in the *s. l.-m.* by perforant glutamatergic input from entorhinal cortex. Synchronous oscillatory inhibition from the basket cells in the perisomatic region constrains pyramidal cell firing while recurrent inhibition from chandelier cells at the axonal initial segment balances recurrent excitation. Shown in the lower right of the figure are the morphologies of Traub's model cells (without their axons for clarity) and where they are situated with respect to the layers of CA3. *s. l.-m.*, stratum lacunosum-moleculare; *s. r.*, stratum radiatum; *s. l.*, stratum lucidum; *s. p.*, stratum pyramidale; *s. o.*, stratum oriens.

NMDA conductances are fixed at 4 nS and 1 nS respectively. Axonal delays are considered negligible and the chandelier cells receive a small hyperpolarizing somatic current injection (0.05 nA) to suppress spontaneous firing.

2.4 Implementation of cholinergic neuromodulation

To study the implications of our model for AD, we have implemented the most prominent of acetylcholine's effects on hippocampal cells: inhibition of intrinsic membrane currents, suppression of excitatory synaptic transmission, and depolarization of membrane potential.

For the inhibition of intrinsic membrane currents we derived dose-response curves based on a Michaelis-Menten model

$$\frac{g_k}{\bar{g}_k} = \frac{a}{1 + \frac{IC_{50}}{[\mathrm{ACh}]}} \tag{3}$$

where g_k is the conductance of ionic current k, $\bar{g}_k$ is the maximal conductance, a is the maximal inhibition, IC_{50} is the concentration that produced half-maximal inhibition, and [ACh] is the concentration of ACh. Nonlinear curve fits matched very closely the data of Madison et al. for I_{AHP} [51] (IC_{50} = 3.0 μM, a = 1.0) and Toselli and Lux for I_{Ca} [66] (IC_{50} = 1.7 μM, a = 0.4). It should be noted that where the original data were collected using either carbachol or muscarine, we have scaled concentrations by a factor of 10 to yield a value for ACh whose effect is diminished by approximately this amount in tissue due to cholinesterase [18].

The suppression of excitatory synaptic transmission in the stratum radiatum (s. r.) and stratum lacunosum-moleculare (s. l.-m.) is based on the data of Hasselmo and colleagues [33, 34]. The logarithmic model

$$\frac{g_{syn}}{\bar{g}_{syn}} = \alpha \log([\mathrm{ACh}]) + \beta \tag{4}$$

gave the best fit to their data yielding α=-0.598, β=2.226 for s. r. and α=-0.176, β=1.352 for s. l.-m. In our simulations, this equation is used to scale both AMPA- and NMDA-mediated EPSCs.

The diffuse cholinergic depolarization of pyramidal and basket cells is modeled indirectly using depolarizing somatic current injection. For basket cells this is represented by setting the DC offset of the "theta" square wave. In the absence of biological data, we have chosen a linear model and scale [ACh] (in μM) by 0.000625 to yield the DC offset in nA. For pyramidal cells [ACh] (in μM) is scaled by 0.016 to give a value for current injection in nA.

Finally, at least one physiological study has shown that the 10μM application of the muscarinic agonist carbachol results in essentially the same effect on pyramidal cells as direct stimulation of muscarinic fibers [51]. As such we have taken 100μM of ACh (or 10μM of carbachol) to be a reasonable approximation of normal physiological conditions.

2.5 Assessing network performance

With 2^{64} possible network states, it is unfeasible to evaluate every possible input to the biological network. In fact, determining the exact state of the network at any given point in time by examining spike traces is a Herculean task. Instead, a compact representation of the network's performance can be given by measuring the overlap or correlation between the current network state and each of the stored patterns as a function of time [1]. The overlap m_p with pattern ξ^p is defined by

$$m_p(t) = 1 - \frac{2d_H(t)}{N} \tag{5}$$

where d_H is the Hamming distance between the current network state and the stored pattern ξ^p. With this metric, an exact match (i.e. the network has reached the attractor state) will give m_p=1 while the inverse of

the stored pattern will give m_p=-1. During the simulations, m_p is calculated for each time step, however, for the figures shown in this paper the sampling filter for simultaneity is 5 ms.

3. Results

3.1 Acetylcholine effects a transition from bursting to spiking

To investigate the possible role of ACh in altering hippocampal network dynamics, we began by investigating its effects on the intrinsic membrane currents of single cells, specifically I_{AHP} and I_{Ca}. Modulation of the muscarinic K^+ current I_M was not simulated because as the contribution of I_M has been reported to be minimal [65] acting mainly to maintain the resting potential of the neuron, and as these channels are thus not present in Traub's model cells. In addition, the simulations described below do not include cholinergic neuromodulation of I_A which, although shown to be inhibited in culture [58], has not been observed using carbachol in the slice preparation [65]. When we have inhibited I_A the only noticeable effect on cellular behavior was a shortening of the depolarizing ramp preceding an action potential (data not shown).

Fig. 3 demonstrates the effect of varying [ACh] for the pyramidal cell model using the dose-response curves derived in the Methods section. Somatically-recorded voltage traces are shown for the same cell using simulated application of 0.1, 0.5, 1, 5, 10, 50, and 100 μM ACh. As [ACh] rises, the cell undergoes a marked transition from low-frequency bursting to high-frequency spiking. In contrast to the pyramidal cell model, the fast spiking of the interneuron model is unaffected by ACh (data not shown). It should be noted, however, that ACh is likely to have different effects on various subpopulations of interneurons [25] due to the differential distribution of receptors and cells across the layers of the hippocampus.

On a qualitative level, the pyramidal cell's transition with respect to its spiking regime can be understood by recognizing that I_{Ca} is responsible for the slow depolarization underlying the burst and the interplay with the fast sodium current that causes the rapid series of action potentials riding the slow depolarization. In contrast, I_{AHP} is the current responsible for terminating the burst and maintaining a long hyperpolarization following it. The inhibition of I_{Ca} by ACh removes the slow calcium-dependentwave, diminishes the reverberating depolarization between soma and adjacent dendrites that create the rapid series of overlying spikes, and affects the calcium dependency of I_{AHP}. The inhibition of I_{AHP} by ACh markedly reduces the afterhyperpolarization that terminates the burst and maintains the low inter-burst interval.

It should also be noted that under these conditions, a very small depolarizing current (0.1 nA) results in a very high spike rate for pyramidal cells as the simulated concentration of ACh rises. In fact, the simulation shown does not take into account the fact that higher levels of ACh would cause even greater depolarization of pyramidal cells and further increasing the spike frequency. However, this rise in spike frequency can be (and in our simulations is) held in check by interneuronal control. Finally, while our simulations demonstrate that cholinergic input is sufficient to induce a transition in pyramidal cell firing mode, Traub and colleagues have shown that tonic somatic current injections [70, 75] or tonic stimulation of slow dendritic $GABA_A$ receptors [70] may be responsible for a similar functional shift. Our results are independent of these two factors as we have held current injection constant at a level that does not induce spiking in the absence of ACh, and we have not included slow dendritic $GABA_A$ receptors.

Such physiological shifts due to muscarinic modulation have been reported in thalamic relay cells [52, 54] and layer V neocortical pyramidal cells [53, 54, 56, 57], while the opposite effect has been noted in GABAergic neurons of the nucleus reticularis of the thalamus [54, 55]. ACh is also believed to induce synchronization in neocortical "chattering" cells [28]. Our results suggest that the cholinergic action in the hippocampus should be similar to that found in the neocortex, but see [6, 48, 64].

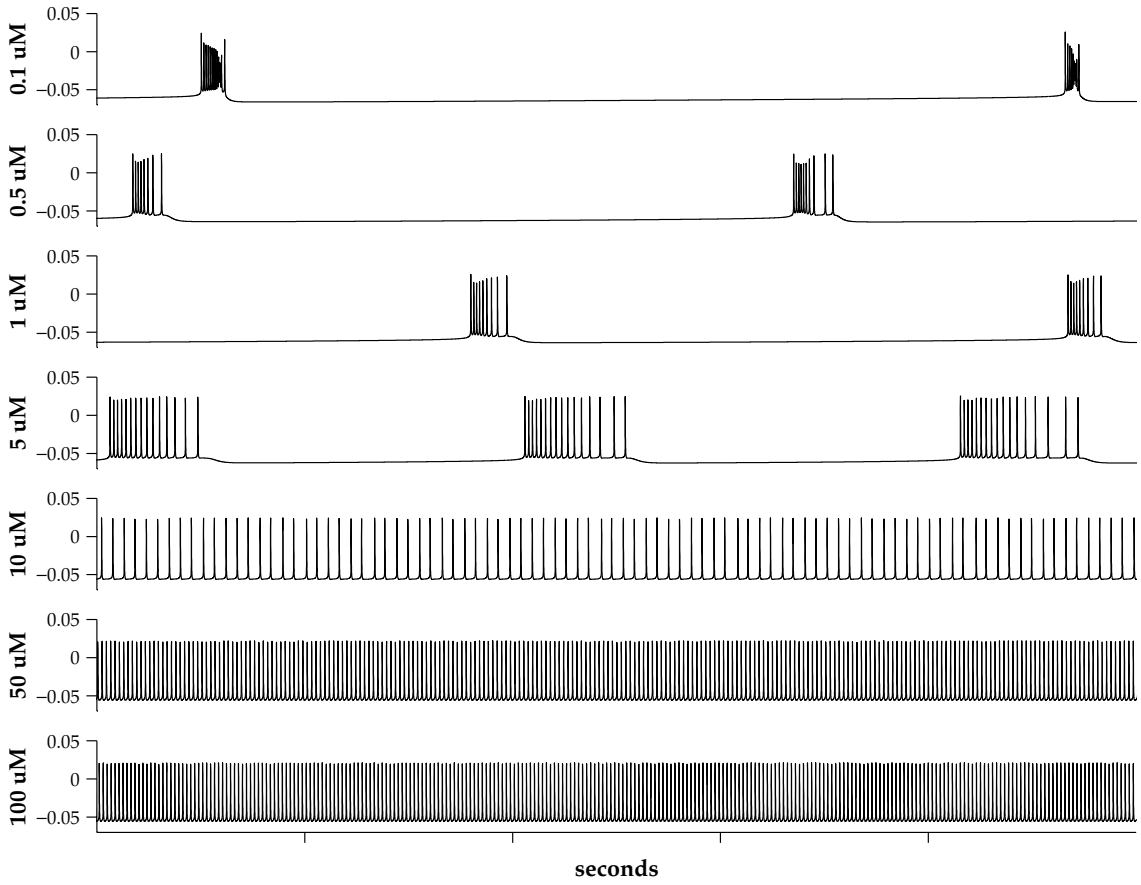

Fig. 3. Muscarinic neuromodulation of a pyramidal cell. Shown are 2.5 seconds of simulated somatic recordings from the model pyramidal cell in the presence of 0.1 to 100 μM ACh. The cell received 0.1 nA current injection in all traces. I_{AHP} and I_{Ca} of the model cell are modulated according to the dose-response curves derived in the Methods section above. At low levels of ACh, the cell still demonstrates its intrinsic low-frequency bursting behavior. As [ACh] rises, there is a marked transition to high-frequency spiking. The same neuromodulation of the interneuron model produces no noticeable change in its fast spiking behavior.

3.2 Spiking vs. Bursting in Pyramidal Cells

In the course of exploring the behavior of the pyramidal cell model under baseline and cholinergic neuromodulatory conditions, we discovered that spiking and bursting in the cell produced very different results with respect to voltage changes and calcium influx in the distal dendrites. As shown in Fig. 4, in the presence of low concentrations of ACh, the bursting pyramidal cell causes a large backpropagating dendritic depolarization with a concomitant influx in dendritic calcium. With the rise of [ACh] and the transition to spiking behavior, backpropagating spikes cause multiple, attenuated depolarizations in the distal dendrite with nearly zero calcium influx. While ACh does inhibit the high-threshold calcium current, even at maximal concentrations the inhibition is only 40% and cannot account for the lack of calcium influx. A more likely candidate for this effect is the differential membrane depolarization; where spiking provides small transient depolarizations of the dendrites, a burst at the soma is transformed into a single large, prolonged depolarization in the arbor.

Given the importance of calcium in signaling the induction and/or maintenance of synaptic plasticity, these results suggest that that spiking may be ill-suited for such a function while bursting could be quite effective. Hence a switch from bursting to spiking (and vice versa) has potentially important consequences for biological networks implementing memory storage and recall. This effect bears some similarity to

results of Antal et al. [2]* in a model of an intrinsically oscillating thalamocortical cell. They observed a modest increase in the size of a slow, backpropagating calcium-based depolarization along with attenuation of sodium-based spikes, however the results were due to the low voltage of the dendrites relative to the soma and the preferential removal of inactivation in dendritic *low-threshold* calcium currents.

3.3 Attractor dynamics in the biological network

Our next step was an investigation of the network's behavior and functional performance under control conditions. The stability of the attractor states (i.e. memories) is demonstrated by presenting each stored memory pattern as input on the perforant pathway and following the evolution of the network state to ensure that it remains at this input state for each successive gamma cycle. Shown in Fig. 5 is the overlap between the network state and each of the five stored memories as a function of time for a single simulation. Each of the stored memories is indeed a fixed point attractor, in spite of the fact that there is considerable overlap between different stored memories (e.g. patterns 4 and 5 can be seen to have a correlation of about 40%). It should be noted that the drop in the overlap for patterns 2 and 5 seen in the last gamma cycle is the intentional disruption of the attractor state by the basket cell population rather than

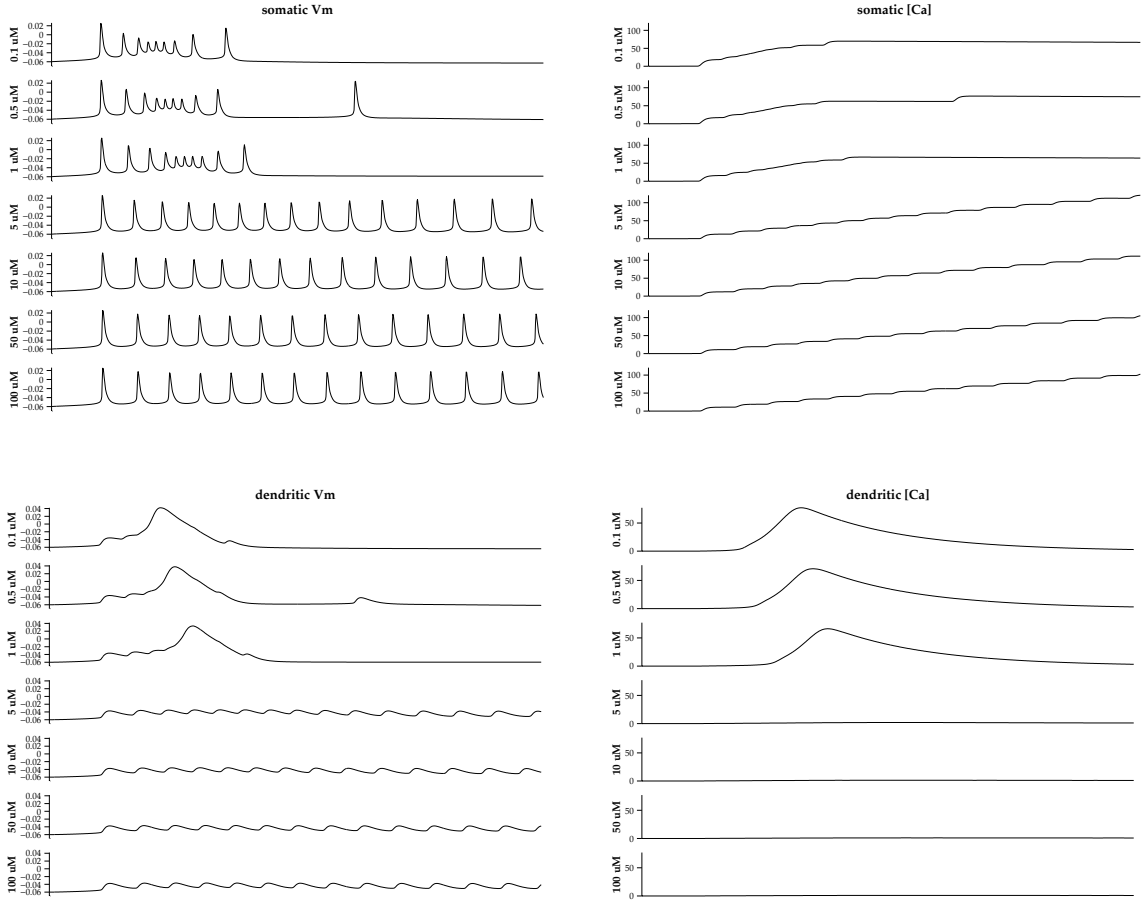

Fig. 4. Comparison of back-propagating spikes and bursts in the hippocampal pyramidal cell model. Shown are 100 ms of voltage and calcium concentration recordings from the soma and a distal dendrite of the pyramidal cell in the presence of a varying amount of ACh. Backpropagating bursts demonstrate a large depolarization of dendritic membrane and induce a large calcium influx. In contrast, backpropagating spikes cause a small depolarization of the dendrite and produce nearly no calcium influx.

* We thank the anonymous reviewer who directed us to this paper.

a defect in network performance. Under these baseline conditions, the gamma rhythm frequency is approximately 100 Hz with 9 gamma cycles used for computation each theta cycle.

Next we tested the recall performance of the network by providing corrupted versions of the stored memories as input and then following the dynamics of the network to see if the proper or any attractor state was reached before the half-way point of the theta cycle. We chose to present degradedinput patterns rather than merely incomplete ones to explore the full capabilities of the network. Corrupted memories were created by randomly flipping some percentage of the bits of the original pattern. The degree of corruption is shown as the overlap between the network state on the first gamma cycle and the stored memory. The top trace of Fig. 6 shows the network dynamics for the presentation of corrupted versions of one of the five stored memories. The correlation between corrupted inputs and the stored memories ranges from 90% down to about 50%, yet the network still reaches the appropriate attractor before the middle of the theta cycle. Thus the network demonstrates error correction as well as recall of memories.

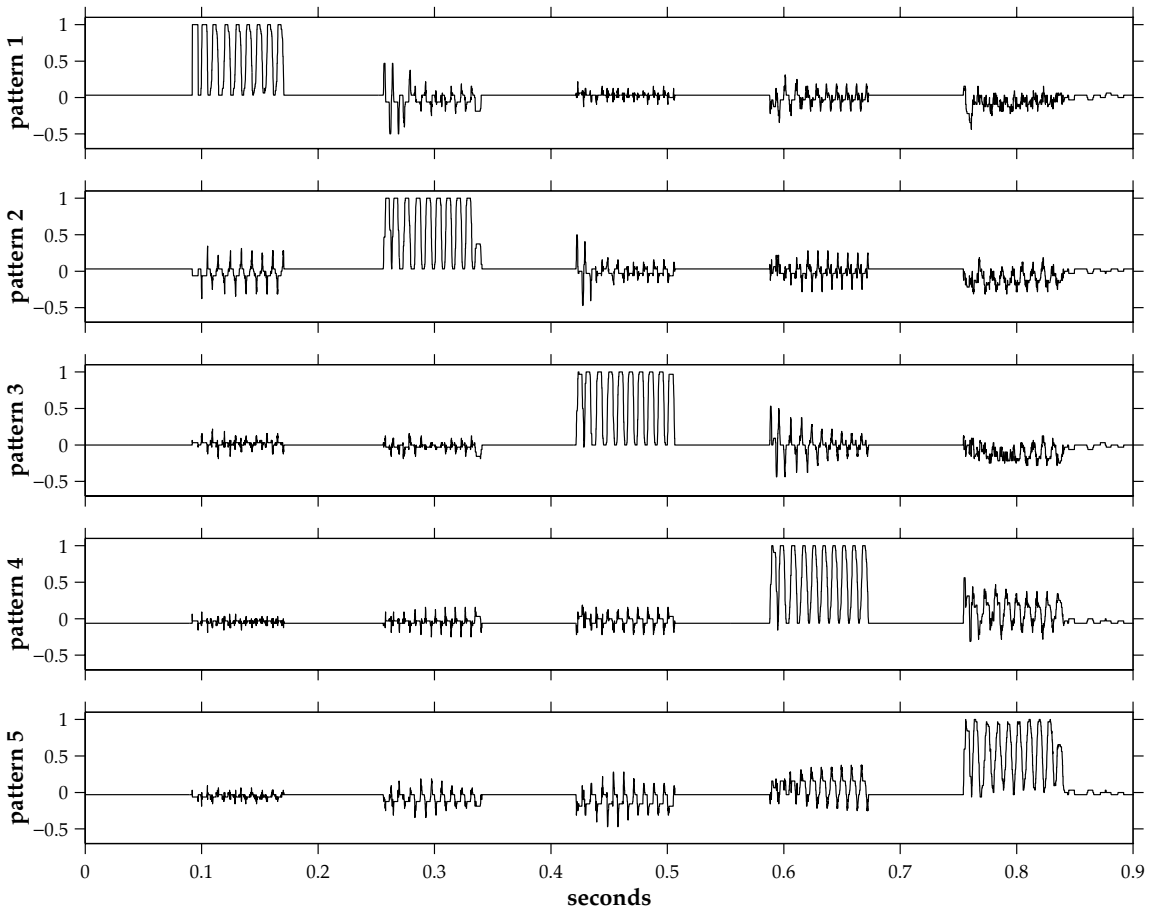

Fig. 5. The stability of attractor dynamics in a realistic CA3 network. The graphs show the value of $m_p(t)$, a measure of the correlation between the current network state (i.e. its spatial distribution of spikes) and the stored memory ξ^p where $m_p(t)$=1.0 is a perfect match. Each of the five stored patterns is presented in sequence to the network by afferent perforant pathway activity at the beginning of each 6 Hz theta cycle (beginning at 83.33 ms and every following 166.67 ms). The function $m_p(t)$ oscillates with each gamma cycle since the pyramidal cells fire synchronously and only once (if at all) during each gamma cycle. Half-way through the theta cycle, when septal inhibition declines, the basket cells begin to fire at high frequency preventing the pyramidal cells from firing. This disruption of the attractor dynamics can be seen as the region where $m_p(t)$=0 between each input presentation. The traces demonstrate that each memory state is, in fact, a basin of attraction; after the first gamma cycle, the network remains in the same state, with overlap equal to 1.0, for all subsequent gamma cycles.

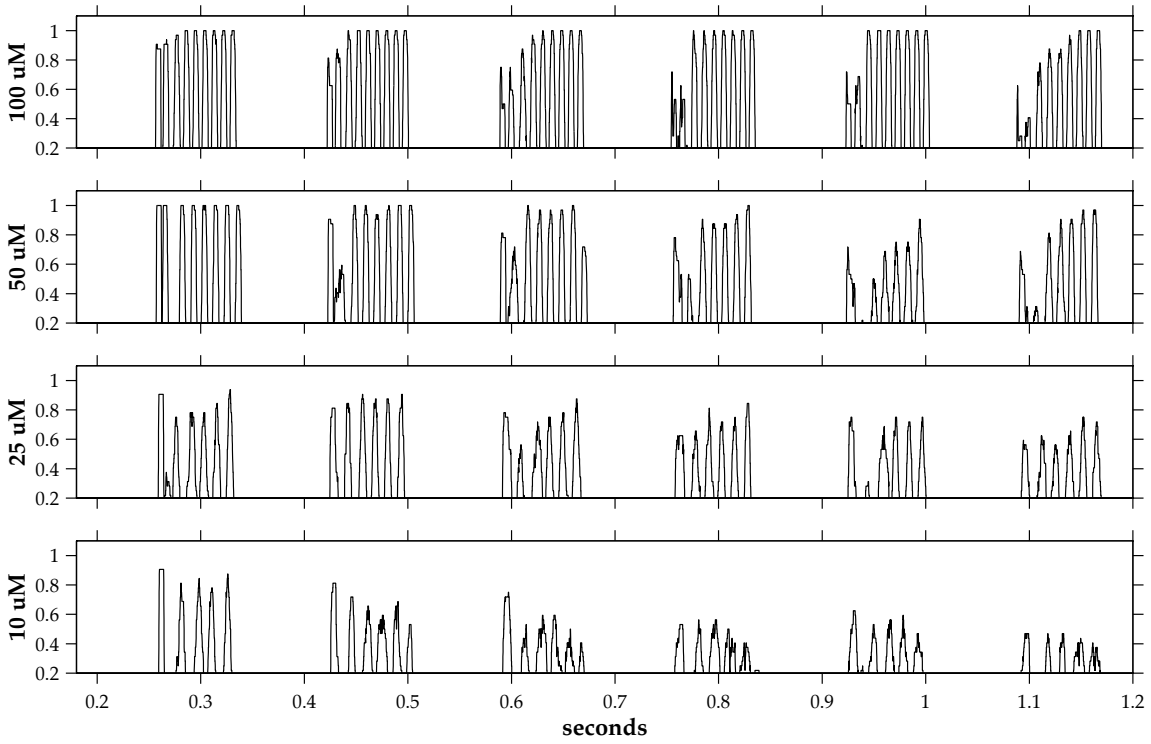

Fig. 6. The decline of cholinergic input and its functional consequences. The overlap plots demonstrate memory reconstruction after presentation of a corrupted or incomplete memory. At the start of each theta cycle, a degraded version of a memory (i.e. 0 < overlap <1) is presented to the network. Over the course of subsequent gamma cycles, the network attempts to recall the uncorrupted memory. The top trace is the baseline condition where even highly degraded input patterns are correctly recalled by the network in only a few gamma cycles. As the [ACh] drops however, the gamma frequency decreases so that the network has fewer cycles with which to reach the attractor state.

3.4 AD-related perturbation of cholinergic neuromodulation

With the baseline performance of the network established, our next step was to examine the effects of a decrease in cholinergic input to CA3, as occurs in AD. Based on the connectivity of the network and the physiology of the cells we had several predictions. First, the network should be robust enough to tolerate a fair range of cholinergic fluctuation due to the balance of excitation and inhibition and the similar effects of ACh on pyramidal cells and interneurons. Second, the decreasing levels of ACh should lead to a lower gamma frequency and therefore fewer gamma cycles per theta cycle. Third, fewer gamma cycles per theta cycle should translate into degraded performance for pattern completion/reconstruction. Finally, we expected that, beyond some point, low levels of ACh would switch pyramidal cells into a bursting regime.

As we expected, the network is quite robust in that it is capable of performing pattern completion/correction on highly degraded input patterns even with [ACh] lowered by 50%. This is demonstrated in the second trace of Fig. 6 where, at 50μM of ACh, the network is still able to reach the appropriate attractor state for various corrupted inputs, but, as predicted, the gamma frequency has dropped so that there are only 7 or 8 gamma cycles per theta cycle. The drop in gamma frequency stems from two sources: 1) decreased depolarization of pyramidal cells and interneurons 2) the increase in both I_{AHP} and I_{Ca} as seen in Fig. 3 causes a lower spike frequency in pyramidal cells for a given depolarization.

As cholinergic input declines even further however, we begin to see diminished network performance. The bottom two traces of Fig. 6 demonstrate the results stemming from further reduction of [ACh] to 25 and 10μM respectively. The gamma frequency continues to drop and eventually the network not only lacks enough gamma cycles to reach the attractor, but its ability to reconstruct the pattern declines as well. This

latter effect appears to be due to the rising strength of the recurrent excitatory synapses which interfere with the correct attractor dynamics.

Our final prediction was that, at very low levels of ACh, the pyramidal cells would revert to their intrinsically bursting mode of firing. This was not immediately apparent for two reasons. First, rising recurrent synaptic activity provided a very strong input to the pyramidal cells that induced spiking similar to the current injection results of Traub et al. [70]. Second, we did not simulate reductions in theta generation (pathological or normal) in the medial septal nuclei. If this effect were included, the disruption of theta generation should disinhibit CA3 basket cells which could then balance the rising recurrent excitation and allow the bursting behavior to re-emerge. This mechanism is likely to play a role in the switch between the functional modes of learning and recall.

4. Discussion

4.1 Comparison with previous computational studies

Although our model is largely inspired by Buzsáki's "two-stage" memory model [15] and his suggested role for interneurons [16], it also bears some resemblance to the model put forth by Lisman and colleagues [45, 50] in its reliance on theta and gamma rhythms. The Lisman model is concerned primarily with storing spatial patterns of spikes as reverberating activity that repeats in the same gamma window of each theta rhythm [50]. The model was later extended to provide for synaptic storage of these patterns and autoassociative recall [45]. Although it is an elegant representation of working memory, we believe this model is not well-suited for clinically-relevant investigations of the hippocampus. The Lisman model is comprised of non-physiological cells defined by algebraic approximations to the appropriate differential equations, thereby removing much of the complexity of actual cells that we sought to control with neuromodulation and interneuronal regulation. An extension of this model to realistic, compartmental cell models proved to be very difficult and highly unconstrained by biological data [21]. Neither the original model nor its compartmental implementation was found to be particularly stable [21]. Finally, the Lisman model's dependenceon reverberating patterns separated by gamma cycles has the restriction that NMDA receptors cannot be used for autoassociative learning. In its stead, Lisman and colleagues have suggested a role for cortical "fast" NMDA receptors [45], but these receptors are not known to exist in the hippocampus.

Over the last several years, two groups have explored the consequences of damage to hippocampal and neocortical networks. The studies of Ruppin and colleagues have focused upon synaptic deletion and compensation in networks of artificial neurons [37, 40-42, 61, 62]. Hasselmo and colleagues have produced a number of studies of cholinergic neuromodulation in both abstracted and realistic network models [4, 5, 31, 33-36]. Coupled with physiological results, Hasselmo's studies have suggested strongly that one function of acetylcholine is to suppress synaptic activity in the stratum radiatum, favoring afferent input in regions CA1 and CA3 and permissive for learning as opposed to recall.

Our model differs in several fundamental ways from those of these two groups. First, we chose to use the most complex hippocampal cellular models available to date in order to best examine the conditions under which biological neurons can be functionally regulated. Second, we have focused on the *cellular* consequences of muscarinic neuromodulation in intrinsically bursting pyramidal cells similar to those populating CA3. Third, we were concerned with the role of interneurons in regulating the functional behavior of pyramidal cells. Fourth, the emerging picture of neurons as much more than simple spatiotemporal integrators [47] led us to explore the implementation of a fast, efficient, *temporally-precise* information coding scheme. Finally, we wished to investigate putative roles for hippocampal theta- and gamma-band synchronous oscillations. Perhaps the strongest contrast is that, based on consideration of the effects of neuromodulation on intrinsic currents, our results suggest that rising levels of ACh should promote network recall rather than learning as Hasselmo et al. have suggested.

4.2 The functional role of spikes and bursts

Physiological recordings show that hippocampal pyramidal cells are capable of either bursting or spiking, and that these different modes are correlated with the behavioral state of the animal. During

exploratory behavior (and REM sleep), hippocampal neurons demonstrate theta- and gamma-band synchronization in both population and single cell recordings. During these states, bursting neurons are almost never seen. In contrast, during consummatory behavior, when theta-band synchronization is absent, bursting neurons are commonly found [71].

From a theoretical perspective, these two firing modes have their respective advantages. Spiking is rapid and can have a temporal precision of a millisecond or so, allowing for efficient representation of information and a well-defined network activity state. However, our simulations have demonstrated that spiking may be poorly suited for inducing and/or maintaining synaptic plasticity in the distal dendritic arbor. Rather, this function appears to be better fulfilled by backpropagating bursts which are capable of causing significant alterations of calcium levels in the dendrites. The drawback for hippocampal bursts lies in their typical low inter-burst frequency and variable length which make the representation of information difficult and inefficient at best.

Together with these behavioral correlations, our findings suggest that spiking behavior is necessary for the initial processing of novel information and its later recall, while bursting is necessary for more permanent storage of patterns via the induction of long-term potentiation and depression. This view is wholly consistent with Buzsáki's "two-stage" memory model in which novel memories are temporarily stored in the hippocampus during the theta-associated behavioral state and more permanently stored with the advent of population bursts that underlie sharp waves [15]. Our model indicates that acetylcholine acts on several levels to initiate and manage a transition from bursting to spiking behavior, at least in intrinsically bursting hippocampal pyramidal cells. At the cellular level, the transition is due to a reduction in the afterhyperpolarizing calcium-dependent potassium current and the high-threshold calcium current.

4.3 The functional CA3 network

The model we have presented is a biological instantiation of the attractor neural network as it was originally proposed by Hopfield [38] and is grounded in hippocampal anatomy and physiology. It utilizes a precise temporal coding scheme for information and suggests putative roles for theta- and gamma-band oscillations. There have been other notable attempts to model the continuous form of the attractor network [1, 39] using a spike frequency representation of information in biophysical network models of neocortex [49] and piriform cortex [4]. We have presented the function of our network with an emphasis on mnemonic function, but one should recognize that the general properties of attractor neural networks make them suitable for the function of spatial navigation as well.

Perhaps the most interesting aspect of this study however arises from the data regarding AD-related cholinergic perturbations. A direct clinical and testable prediction arising from our model is that the progression of AD and its associated destruction of cholinergic cells in the medial septum and diagonal band of Broca should correlate with decreased frequency of the gamma rhythm during recall of recent memories (i.e. those stored in CA3 as opposed to those in long-term storage elsewhere in cortex). This reduction in gamma frequency should correlate with impaired mnemonic recall. In addition, the investigation of attractor states related to gamma and theta rhythms should be amenable to physiological study using multiple-electrode recordings in the near future if not today.

It should be noted that the results presented here are of a preliminary nature. Perhaps the greatest deficit in the current model is the lack of synaptic plasticity and a learning stage. While this absence is not biologically sound, we feel that it actually argues in favor of the model rather than against it. Given the complexity of the individual cells, if this crude approximation of a synaptic matrix is sufficient to store memories that are recalled rapidly and robustly, it is even more likely that a synaptic matrix custom crafted by Hebbian learning will perform even better.

A second obvious implausibility is the proportion of pyramidal cells to interneurons which should be closer to 10:1. This direct mapping of the Hopfield paradigm to compartmental cell models required a single interneuron to perform recurrent inhibition for each pyramidal cell in the network. Interestingly, under the appropriate conditions, a formal attractor model can function quite well with a single, global source of inhibition (J. Hopfield, personal communication).

4.4 AD as a disease of neuromodulation

Several studies have shown a strong correlation between the loss of synapses in AD and measurable deficits in cognitive function. However, with the human CA3 region comprising some 2.3 million cells [13] and employing a distributed information coding scheme, the performance of the CA3 network should be relatively robust in the face of low to moderate levels of neuronal loss. In contrast, the loss of subcortical neurons in neuromodulatory nuclei (e.g. the medial septal nuclei, the locus coeruleus, the dorsal and median raphe nuclei) could rapidly lead to defects in the regulation of hippocampal cells and a subsequent impact on mnemonic function. This is particularly true for the CA3 region which is spared much of the early AD-related neuropathology [3].

Although this and other computational studies of AD have focused upon the cholinergic hypothesis of AD, it should be kept in mind that a palette of neuromodulatory substances are involved in hippocampal function including norepinephrine, serotonin, dopamine, histamine, GABA (via $GABA_B$ receptors), glutamate (via metabotropic receptors), adenosine, neuropeptide Y, and corticotropin releasing factor. More important than the absolute concentrations of individual neuromodulators may be the relative concentrations of multiple agents, the dynamics of their concentrations, and the differential dose-response characteristics for independent effects of a single neuromodulator. In addition to AD, studies of neuromodulatory control in the central nervous system have great potential for providing critical insights into numerous CNS disorders including epilepsy, Parkinson's disease, and schizophrenia to name but a few [20].

5. Acknowledgments

We thank Dr. Howard Crystal for his review of this manuscript, his suggestions and useful discussions of Alzheimer's disease. Supported by grants from The Patricia Kind Foundation, The Whitaker Foundation, Office of Naval Research, and the McDonnell-Pew Program in Cognitive Neuroscience.

References

[1] D. J. Amit, *Modeling Brain Function: The world of attractor neural networks* (Cambridge University Press, New York, 1989).

[2] K. Antal, Z. Emri, T. I. Toth and V. Crunelli, Model of a thalamocortical neurone with dendritic voltage-gated ion channels, *Neuroreport 7* (1996) 2655-2658.

[3] S. E. Arnold, B. T. Hyman, J. Flory, A. R. Damasio and G. W. Van Hoesen, The topographical and neuroanatomical distribution of neurofibrillary tangles and neuritic plaques in the cerebral cortex of patients with Alzheimer's disease, *Cerebral Cortex 1* (1991) 103-116.

[4] E. Barkai, R. E. Bergman, G. Horwitz and M. E. Hasselmo, Modulation of associative memory function in a biophysical simulation of rat piriform cortex, *Journal of Neurophysiology 72* (1994) 659-677.

[5] E. Barkai and M. E. Hasselmo, Modulation of the input/output function of rat piriform cortex pyramidal cells, *Journal of Neurophysiology 72* (1994) 644-658.

[6] L. S. Benardo and D. A. Prince, Acetylcholine induced modulation of hippocampal pyramidal neurons, *Brain Research 211* (1981) 227-234.

[7] D. Benson, R. D. Blitzer and E. M. Landau, An analysis of the depolarization produced in guinea pig hippocampus by cholinergic receptor stimulation, *Journal of Physiology (London) 404* (1988) 479-496.

[8] D. M. Bowen, J. S. Benton, J. A. Spillane, C. C. Smith and S. J. Allen, Choline acetyltransferase activity and histopathology of frontal neocortex from biopsies of demented patients, *Journal of the Neurological Sciences 57* (1982) 191-202.

[9] J. M. Bower and D. Beeman, *The Book of GENESIS: Exploring Realistic Neural Models with the GEneral NEural SImulation System* (TELOS/Springer-Verlag, Santa Clara, CA, 1994).

[10] H. Braak and E. Braak, Neuropathological stageing of Alzheimer-related changes, *Acta Neuropathologica 82* (1991) 239-259.

[11] D. A. Brown and P. R. Adams, Muscarinic suppression of a novel voltage-sensitive K+ current in a vertebrate neurone, *Nature (London) 283* (1980) 673-676.

[12] D. A. Brown, S. Nakajima and Y. Nakajima, Acetylcholine modulates resting K-current through a pertussis toxin-resistant G-protein in hippocampal neurons, *Society for Neuroscience Abstracts 14* (1988) 1328.

[13] M. W. Brown and M. D. Cassell, Estimates of the number of neurones in the human hippocampus, *Journal of Physiology 301* (1980) 58P-59P.

[14] P. Bush and T. J. Sejnowski, Inhibition synchronizes sparsely connected cortical neurons within and between columns in realistic network models, *Journal of Computational Neuroscience 3* (1996) 91-110.
[15] G. Buzsáki, Two-stage model of memory trace formation: a role for "noisy" brain states, *Neuroscience 31* (1989) 551-570.
[16] G. Buzsáki and J. J. Chrobak, Temporal structure in spatially organized neuronal ensembles: A role for interneuronal networks, *Current Opinion in Neurobiology 5* (1995) 504-510.
[17] A. E. Cole and R. A. Nicoll, Acetylcholine mediates a slow synaptic potential in hippocampal pyramidal cells, *Science 221* (1983) 1299-1301.
[18] A. E. Cole and R. A. Nicoll, Characterization of a slow cholinergic post-synaptic potential recorded in vitro from rat hippocampal pyramidal cells, *Journal of Physiology 352* (1984) 173-188.
[19] A. E. Cole and R. A. Nicoll, The pharmacology of cholinergic excitatory responses in hippocampal pyramidal cells, *Brain Research 305* (1984) 283-290.
[20] H. Crystal and L. H. Finkel, Computational Approaches to Neurological Disease, in J. A. Reggia, E. Ruppin and R. Sloan Berndt, eds., *Neural Modeling of Brain and Cognitive Disorders* (World Scientific, Singapore, 1996).
[21] H. A. Crystal, E. D. Menschik and L. H. Finkel, Biophysically Realistic Models of Working Memory, in J. Bower, ed., *Proceedings of the 6th Annual Conference on Computational Neuroscience* (Big Sky, Montana, July 6-10, 1997)
[22] P. Davies and A. J. Maloney, Selective loss of central cholinergic neurons in Alzheimer's disease, *Lancet 2* (1976) 1403.
[23] D. A. Drachman, Memory and cognitive function in man: does the cholinergic system have a specific role?, *Neurology 27* (1977) 783-790.
[24] R. Fisher and D. Johnston, Differential modulation of single voltage-gated calcium channels by cholinergic and adrenergic agonists in adult hippocampal neurons, *Journal of Neurophysiology 64* (1990) 1291-1302.
[25] T. F. Freund and G. Buzsáki, Interneurons of the Hippocampus, *Hippocampus 6* (1996) 345-470.
[26] B. H. Gahwiler and D. A. Brown, Muscarine affects calcium-currents in rat hippocampal pyramidal cells in vitro, *Neuroscience Letters 76* (1987) 301-306.
[27] N. H. Goddard and G. Hood, Large Scale Simulation with PGENESIS, in J. M. Bower and D. Beeman, eds., *The Book of GENESIS: Exploring Realistic Neural Models with the GEneral NEural SImulation System* (Springer-Verlag, in press).
[28] C. M. Gray and D. A. McCormick, Chattering cells: superficial pyramidal neurons contributing to the generation of synchronous oscillations in the visual cortex, *Science 274* (1996) 109-113.
[29] M. E. Hasselmo, Neuromodulation and cortical function: modeling the physiological basis of behavior, *Behavioural Brain Research 67* (1995) 1-27.
[30] M. E. Hasselmo, B. P. Anderson and J. M. Bower, Cholinergic modulation of cortical associative memory function, *Journal of Neurophysiology 67* (1992) 1230-1246.
[31] M. E. Hasselmo and E. Barkai, Cholinergic modulation of activity-dependent synaptic plasticity in the piriform cortex and associative memory function in a network biophysical simulation, *Journal of Neuroscience 15* (1995) 6592-6604.
[32] M. E. Hasselmo and J. M. Bower, Cholinergic suppression specific to intrinsic not afferent fiber synapses in rat piriform (olfactory) cortex, *Journal of Neurophysiology 67* (1992) 1222-1229.
[33] M. E. Hasselmo and E. Schnell, Laminar selectivity of the cholinergic suppression of synaptic transmission in rat hippocampal region CA1: computational modeling and brain slice physiology, *Journal of Neuroscience 14* (1994) 3898-3914.
[34] M. E. Hasselmo, E. Schnell and E. Barkai, Dynamics of learning and recall at excitatory recurrent synapses and cholinergic modulation in rat hippocampal region CA3, *Journal of Neuroscience 15* (1995) 5249-5262.
[35] M. E. Hasselmo and B. P. Wyble, Does the spread of Alzheimer's disease neuropathology involve the mechanisms of consolidation?, in J. A. Reggia, E. Ruppin and R. Sloan Berndt, eds., *Neural Modeling of Brain and Cognitive Disorders* (World Scientific, River Edge, NJ, 1996).
[36] M. E. Hasselmo, B. P. Wyble and G. V. Wallenstein, Encoding and retrieval of episodic memories: Role of Cholinergic and GABAergic modulation in the hippocampus, *Hippocampus 6* (1996) 693-708.
[37] M. Herrmann, E. Ruppin and M. Usher, A neural model of the dynamic activation of memory, *Biological Cybernetics 68* (1993) 455-463.
[38] J. J. Hopfield, Neural networks and physical systems with emergent collective computational abilities, *Proceedings of the National Academy of Sciences of the United States of America 79* (1982) 2554-2558.
[39] J. J. Hopfield, Neurons with graded response have collective computational properties like those of two-state neurons, *Proceedings of the National Academy of Sciences of the United States of America 81* (1984) 3088-3092.

[40] D. Horn, N. Levy and E. Ruppin, Neural-network modeling of memory deterioration in Alzheimer's disease, *Neural Computation 5* (1993) 736-749.
[41] D. Horn, N. Levy and E. Ruppin, Neuronal-based synaptic compensation: a computational study in Alzheimer's disease, *Neural Computation 8* (1996) 1227-1243.
[42] D. Horn and E. Ruppin, Extra-pyramidal symptoms in Alzheimer's disease: a hypothesis, *Medical Hypotheses 39* (1992) 316-318.
[43] J. Hounsgaard, Presynaptic inhibitory action of acetylcholine in area CA1 of the hippocampus, *Experimental Neurology 62* (1978) 787-797.
[44] B. T. Hyman, G. W. Van Hoesen and A. R. Damasio, Memory-related neural systems in Alzheimer's disease: an anatomic study, *Neurology 40* (1990) 1721-1730.
[45] O. Jensen, M. A. P. Idiart and J. E. Lisman, Physiologically realistic formation of autoassociative memory in networks with theta/gamma oscillations -- Role of fast NMDA channels, *Learning and Memory 3* (1996) 243-256.
[46] R. Katzman, Alzheimer's disease, *New England Journal of Medicine 314* (1986) 964-973.
[47] P. König, A. K. Engel and W. Singer, Integrator or coincidence detector? The role of the cortical neuron revisited, *Trends in Neurosciences 19* (1996) 130-137.
[48] A. R. Kriegstein, T. Suppes and D. A. Prince, Cholinergic enhancement of penicillin-induced epileptiform discharges in pyramidal neurons of the guinea pig hippocampus, *Brain Research 266* (1983) 137-142.
[49] A. Lansner and E. Fransén, Modeling Hebbian Cell Assemblies Comprised of Cortical Neurons, *Network 3* (1992) 105-119.
[50] J. E. Lisman and M. A. Idiart, Storage of 7 +/- 2 short-term memories in oscillatory subcycles, *Science 267* (1995) 1512-1515.
[51] D. V. Madison, B. Lancaster and R. A. Nicoll, Voltage clamp analysis of cholinergic action in the hippocampus, *Journal of Neuroscience 7* (1987) 733-741.
[52] D. A. McCormick, Cellular mechanisms underlying cholinergic and noradrenergic modulation of neuronal firing mode in the cat and guinea pig dorsal lateral geniculate nucleus, *Journal of Neuroscience 12* (1992) 278-289.
[53] D. A. McCormick, Neurotransmitter actions in the thalamus and cerebral cortex and their role in neuromodulation of thalamocortical activity, *Progress in Neurobiology 39* (1992) 337-388.
[54] D. A. McCormick, Actions of acetylcholine in the cerebral cortex and thalamus and implications for function, *Progress in Brain Research 98* (1993) 303-308.
[55] D. A. McCormick and D. A. Prince, Acetylcholine induces burst firing in thalamic reticular neurones by activating a potassium conductance, *Nature 319* (1986) 402-405.
[56] D. A. McCormick and D. A. Prince, Mechanisms of action of acetylcholine in the guinea-pig cerebral cortex in vitro, *Journal of Physiology 375* (1986) 169-194.
[57] D. A. McCormick, Z. Wang and J. Huguenard, Neurotransmitter control of neocortical neuronal activity and excitability, *Cerebral Cortex 3* (1993) 387-398.
[58] Y. Nakajima, S. Nakajima, R. J. Leonard and K. Yamaguchi, Acetylcholine raises the excitability by inhibiting the fast transient outward current in cultured hippocampal neurons, *Proceeding of the National Academy of Science, USA 83* (1986) 3022-3026.
[59] D. L. Price, New perspectives on Alzheimer's disease, *Annual Review of Neuroscience 9* (1986) 489-512.
[60] L. J. Reece and P. A. Schwartzkroin, Effects of cholinergic agonists on two non-pyramidal cell types in rat hippocampal slices, *Brain Research 566* (1991) 115-126.
[61] E. Ruppin, D. Horn, N. Levy and J. A. Reggia, Computational studies of synaptic alterations in Alzheimer's disease, in J. A. Reggia, E. Ruppin and R. Sloan Berndt, eds., *Neural Modeling of Brain and Cognitive Disorders* (World Scientific, River Edge, NJ, 1996).
[62] E. Ruppin and J. A. Reggia, Patterns of functional damage in neural network models of associative memory, *Neural Computation 7* (1995) 1105-1127.
[63] D. J. Selkoe, Physiological production of the beta-amyloid protein and the mechanism of Alzheimer's disease, *Trends in Neurosciences 16* (1993) 403-409.
[64] M. Stewart, Y. Luo and S. E. Fox, Effects of atropine on hippocampal theta cells and complex-spike cells, *Brain Research 591* (1992) 122-128.
[65] J. F. Storm, Potassium currents in hippocampal pyramidal cells, *Progress in Brain Research 83* (1990) 161-187.
[66] M. Toselli and H. D. Lux, GTP-binding proteins mediate acetylcholine inhibition of voltage dependent calcium channels in hippocampal neurons, *Pflugers Archiv - European Journal of Physiology 413* (1989) 319-321.

[67] M. Toselli and H. D. Lux, Opposing effects of acetylcholine on the two classes of voltage-dependent calcium channels in hippocampal neurons, *Exs 57* (1989) 97-103.
[68] M. Toselli and V. Taglietti, Muscarinic inhibition of high-voltage-activated calcium channels in excised membranes of rat hippocampal neurons, *European Biophysics Journal 22* (1994) 391-398.
[69] M. Toselli and V. Taglietti, Muscarine inhibits high-threshold calcium currents with two distinct modes in rat embryonic hippocampal neurons, *Journal of Physiology 483* (1995) 347-365.
[70] R. D. Traub, J. G. R. Jefferys, R. Miles, M. A. Whittington and K. Tóth, A branching dendritic model of a rodent CA3 pyramidal neurone, *Journal of Physiology 481* (1994) 79-95.
[71] R. D. Traub and R. Miles, *Neuronal Networks of the Hippocampus* (Cambridge University Press, New York, 1991).
[72] R. D. Traub and R. Miles, Pyramidal cell-to-inhibitory cell spike transduction explicable by active dendritic conductances in inhibitory cell, *Journal of Computational Neuroscience 2* (1995) 291-298.
[73] R. D. Traub, M. A. Whittington, S. B. Colling, G. Buzsáki and J. G. R. Jefferys, Analysis of gamma rhythms in the rat hippocampus in vitro and in vivo, *Journal of Physiology 493* (1996) 471-484.
[74] R. D. Traub, M. A. Whittington, I. M. Stanford and J. G. R. Jefferys, A mechanism for generation of long-range synchronous fast oscillations in the cortex, *Nature 383* (1996) 621-624.
[75] R. D. Traub, R. K. Wong, R. Miles and H. Michelson, A model of a CA3 hippocampal pyramidal neuron incorporating voltage-clamp data on intrinsic conductances, *Journal of Neurophysiology 66* (1991) 635-650.
[76] A. Treves and E. T. Rolls, Computational analysis of the role of the hippocampus in memory, *Hippocampus 4* (1994) 374-391.
[77] R. J. Valentino and R. Dingeldine, Presynaptic inhibitory effect of acetylcholine in the hippocampus, *Journal of Neuroscience 1* (1981) 784-792.
[78] O. S. Vinogradova, Expression, control, and probable functional significance of the neuronal theta-rhythm, *Progress in Neurobiology 45* (1995) 523-583.
[79] X. J. Wang and G. Buzsáki, Gamma oscillation by synaptic inhibition in a hippocampal interneuronal network model, *Journal of Neuroscience 16* (1996) 6402-6413.
[80] P. J. Whitehouse and J. R. Unnerstall, Neurochemistry of dementia, *European Neurology 28* (1988) 36-41.
[81] G. K. Wilcock, M. M. Esiri, D. M. Bowen and A. O. Hughes, The differential involvement of subcortical nuclei in senile dementia of Alzheimer's type, *Journal of Neurology, Neurosurgery & Psychiatry 51* (1988) 842-849.